High-Energy X-ray Radiation Registration Model

S P Osipov[1], O S Osipov[2], and K V Ignatenko[3]

[1]Leading Researcher, National Research Tomsk Polytechnic University, Tomsk, Russia
[2]Programmer, Company Solveig Multimedia, Tomsk, Russia
[3]Graduate Student, National Research Tomsk Polytechnic University, Tomsk, Russia

E-mail: osip1809@rambler.ru

Abstract. It is proved the necessity for carrying out computing experiments according to the mean value and the square of registered X-ray photons absorbed energy of in a scintillation detector. The offered imitation model of the transfer and registration of high-energy X-ray radiation in a sensing volume of CsI and $CdWO_4$ scintillation detectors is based on a Monte Carlo method. The model considers leakage of secondary photons and electrons. It is offered approaches to justification of adequacy of the developed model of a high-energy X-ray radiation registration.

1. Introduction

The present period is characterized by rapid systems development of digital radiography (DR), computed tomography (CT) and their applications [1, 2]. Non-destructive tests and customs monitoring of large-size objects by digital radiography and a computer tomography methods are impossible without sources of high-energy X-ray radiation. Betatrons and linacs of electrons are used as sources of X-ray photons with high maximal energy [3−6]. The main consumer characteristics of DR and CT systems are sensitivity, spatial resolution and efficiency. In the analyzed systems, rulers or matrixes of radiometric detectors, scintillation screens (panels) interfaced to a matrix of photo-detectors are applied as registrars of X-ray emission [7]. If elementary detectors of the linear and matrix registrars of radiation are isolate, and the radiating surface of photons sources has the small dimensions, then geometrical resolution of DR and CT systems is determined by detector sizes in the direction of perpendicular to a stream of quanta. Isolation is understood as absence or insignificance of optical and radiation interconnection of the next detectors. Optical signal interconnection from the next photo-detectors can be very significant for panel registrars. For this case, geometrical resolution of analyzed systems can be essentially less than the size of a contact surface of an elementary photo-detector. Effectiveness of filing of any kinds of registrars of X-ray radiation is determined by corresponding sensing volumes thickness in the direction of radiation propagation. Increase in thickness of scintillation screens conflicts with need of increase in geometrical resolution. Increasing the thickness of sensing volumes of elementary detectors is technologically difficult task for linear and matrix registrars of X-ray radiation. Thus, technical and technological correctness of using small effective sensing volumes of radiation and optical converters follows from the analysis of geometrical parameters of modern registrars of high-energy X-ray radiation. It is emphasized in the work [8] that high-energy X-ray photons leave a small part of energy when interacting with a scintillator that has small thickness or small cross sectional dimensions. Another part of photons energy is absorbed in the

next detectors or transferred to external space. Secondary photons and electrons have high penetration ability therefore for primary interaction their filing not in the detector leads to deterioration in geometrical resolution of DR and CT systems. Measuring simple radiometric signals and appropriate noise levels remains one of the most important design problems of analyzed test systems. Calculation data of mean value and mean square dependences of registered photon absorbed energy by cylindrical scintillator radius based on various materials without regard to leakage of secondary electrons are given in the article [9]. An approach for approximating secondary electrons leakage is offered in the work [10]. The data obtained in the works [9, 10] are enough to estimate the mean value and the mean square of the registered photon absorbed energy for scintillation detectors which radius and thickness are more than 5 mm. For modern registrars of high-energy X-ray radiation, these data need to be corrected. The experimental solution of this problem is impossible because of a large number of parameters and high material cost. It means there is no alternatives to the modeling the X-ray radiation transfer by Monte Carlo method.

2. The Model of Photon Transfer Process in a Scintillator
The model of X-ray photons transfer in a substance by Monte Carlo method is based on the algorithms from the work [11] enhanced by blocks of secondary electron interactions with scintillator material.

2.1. Data for the Model
Assume infinitely thin X-ray radiation beam with continuous ionization energy spectrum falls along the axis on cylindrical scintillators with the radius r and thickness h. Scintillator material is CsI, $CdWO_4$. The classical Schiff's formula [12] is used for the description of high-energy spectra of X-ray radiation sources, various approximations are described in details in the article [13]. X-ray radiation maximal energies vary from 2 to 10 MeV. All main interaction effects of photons and substance considered in the model are as follows: the photo-effect, the coherent and incoherent scattering, the pair creation effect. The investigated random variable is the amount of absorbed energy left in a scintillator experienced interaction with a photon. Energy transfer of secondary photons and electrons is taken into account. The considered trajectories number N is set by a user.

2.2. Formation of the Preliminary Data
For increasing algorithm performance, the user database is formed at a preliminary stage on the base of 127-group library of data of interaction between gamma radiation and substance [14]. The data library [14] is a table of energy dependence of the total cross section of X-ray radiation interactions with substance $\sigma_{tot}(E_i)$ and interaction sections for photo-effect $\sigma_{foto}(E_i)$, Compton scattering $\sigma_C(E_i)$, Rayleigh scattering $\sigma_K(E_i)$ and pair creation $\sigma_{par}(E_i)$; the variable i varies from 1 to 127. The corresponding tables of the linear extinction coefficients $\mu_{tot}(E_i)$, $\mu_{foto}(E_i)$, $\mu_C(E_i)$, $\mu_K(E_i)$ and $\mu_{par}(E_i)$ are formed for the analyzed types of scintillators at the first stage. The user database consists of the spline-interpolation coefficients: a_i, b_i, c_i, d_i for the energy dependence $\mu_{tot}(E_i)$; $a_{foto\ i}$, $b_{foto\ i}$, $c_{foto\ i}$, $d_{foto\ i}$ for $\mu_{foto}(E_i)$; $a_{C\ i}$, $b_{C\ i}$, $c_{C\ i}$, $d_{C\ i}$ for $\mu_C(E_i)$; $a_{K\ i}$, $b_{K\ i}$, $c_{K\ i}$, $d_{K\ i}$ for $\mu_K(E_i)$; $a_{par\ i}$, $b_{par\ i}$, $c_{par\ i}$, $d_{par\ i}$ for $\mu_{par}(E_i)$. Furthermore, approximating functions which cumulative distribution functions of energy of E inverse to $F(E)$ considered as a random value are included in the user database. The table of the function $F(E)$ is calculated from the approximations [12, 13] of the numerical energy distribution $f(E, E_{max})$ for a X-ray radiation source with the maximal energy E_{max}

$$F(E) = \int_0^{E_{max}} f(E, E_{max})\,dE \,. \tag{1}$$

Further, the table of the function $F^{-1}(E)$ is constructed from the table of the function $F(E)$. Let's notice that partitioning the energy range should not be more frequent than in the library [14]. Table spline-interpolation coefficients of the function $F^{-1}(E)$ are included to the user database: a_{fj}, b_{fj}, c_{fj}, d_{fj}.

2.3. Algorithm of the model of radiation transfer in a scintillator

The transfer model algorithm by Monte Carlo method comes down to the uniform draw of the trajectories with the same origin. The standard geometrical scheme of a draw of photon radiation transfer in a scintillator is represented in the figure 1 with the corresponding coordinate axis *XOY*. For convenience, let's consider polar coordinate axis with a lateral angle ω and a polar angle ψ. The red continuous line marks the trajectory of the primary photon. The red dash line marks the trajectory of the secondary photon. There are no such photons for the case of photo-effect, and there are exactly two photons with identical energy 0.511 MeV for the case of pair creation.

The secondary photon energy coincides with the primary photon energy for Rayleigh scattering but differs by the direction. The green marks a trajectory of a secondary electron on the Figure 1. For convenient, let's consider the auxiliary polar coordinate axis corresponded to the initial axis. The polar angles θ and $\theta\,'$ determine the difference between the primary photon and secondary particle directions (for a photon or for an electron). The corresponding azimuthal angles φ and $\varphi\,'$ are equal to the angle between the vector's projection of the secondary particle movement to the plane *X'O'Y'* and *O'X* axis.
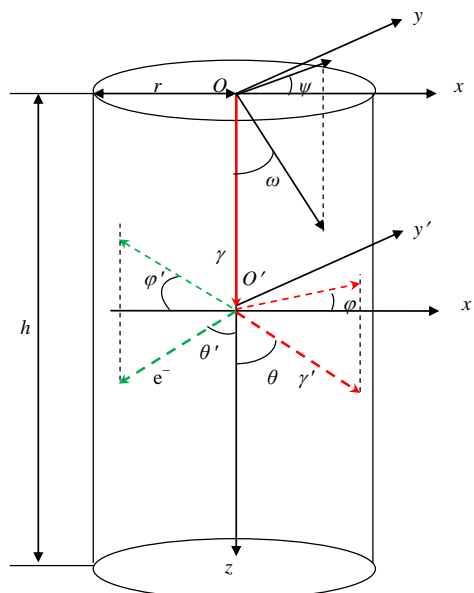

Figure 1. The geometrical scheme of a draw of photon radiation transfer in a scintillator

The surface of the cylindrical scintillator *S* is described by the expression

$$\mathbf{S} = \left\{ (x, y, z) : \begin{array}{l} x^2 + y^2 = r^2,\ 0 < z < h, \\ x^2 + y^2 \le r^2,\ z = 0 \vee z = h \end{array} \right\}. \tag{2}$$

For increasing calculation efficiency, the corresponding averages were applied at each stage of photon interaction with scintillator material. Stages of the algorithm make a short list.

Zeroing of the photon counter $i=0$, the adders of the absorbed energy $\sum E_{ab}$ and the square of the absorbed energy $\sum E_{ab}^2$.

1. Cartesian and polar coordinates of photon penetration into a scintillator and coordinates *a*, *b*, *c* of a unit vector of the photon direction and weight factor *w* are as follows

$$\begin{cases} x = 0 \\ y = 0 \\ z = 0 \end{cases} \quad \begin{cases} \omega = 0 \\ \psi = 0 \end{cases} \quad \begin{cases} a = \sin\omega\cos\psi = 0 \\ b = \sin\omega\sin\psi = 0 \quad w = 1. \\ c = \cos\omega = 1 \end{cases} \tag{3}$$

2. Increasing the photon counter: $i=i+1$. Zeroing the interaction counter: $k=0$. Zeroing the local adder of the absorbed energy and the square of the absorbed energy of one registered photon: $E_{ab}=0$. A draw of photon energy by the method of inverse functions is given by the formula

$$E = F^{-1}(\xi) = \mathrm{spline}(\mathbf{a}_f, \mathbf{b}_f, \mathbf{c}_f, \mathbf{d}_f, \xi), \tag{4}$$

where $\mathbf{a}_f$, $\mathbf{b}_f$, $\mathbf{c}_f$, $\mathbf{d}_f$ are columns of spline interpolation parameters for approximation of the function F^{-1}; ξ is a random number with uniform distribution from 0 to 1; spline is a function returning the value of the spline.

3. Calculating the linear extinction coefficients $\mu_{tot}(E)$, $\mu_{foto}(E)$, $\mu_C(E)$, $\mu_K(E)$ and $\mu_{par}(E)$:

$$\begin{aligned}\mu_{tot}(E) &= \mathrm{spline}(\mathbf{a}_{tot}, \mathbf{b}_{tot}, \mathbf{c}_{tot}, \mathbf{d}_{tot}, E) \quad \mu_{foto}(E) = \mathrm{spline}(\mathbf{a}_{foto}, \mathbf{b}_{foto}, \mathbf{c}_{foto}, \mathbf{d}_{foto}, E) \\ \mu_C(E) &= \mathrm{spline}(\mathbf{a}_C, \mathbf{b}_C, \mathbf{c}_C, \mathbf{d}_C, E) \qquad \mu_{par}(E) = \mathrm{spline}(\mathbf{a}_{par}, \mathbf{b}_{par}, \mathbf{c}_{par}, \mathbf{d}_{par}, E)\end{aligned} \tag{5}$$

4. Determining the coordinates of the hypothetical quantum exit from the scintillator as intersection point with the surface S the straight line given by the formula:

$$\begin{cases} x_h = x + al_h \\ y_h = y + bl_h \\ z_h = z + cl_h \end{cases}, \tag{6}$$

where l_h is the distance from the interaction point (entrance) to the point of photon's hypothetical departure from the scintillator.

5. Drawing a photon run on condition of its interaction before the departure point, correction of the weight factor and the interaction counter:

$$l = -\frac{1}{\mu_{tot}(E)}\ln\left(1 - \xi\left(1 - e^{-\mu_{tot}(E)l_h}\right)\right), \quad w = w\left(1 - e^{-\mu_{tot}(E)l_h}\right), k = k+1. \tag{7}$$

6. Calculating the coordinates of the interaction point:

$$\begin{cases} x = x + al \\ y = y + bl \\ z = z + cl \end{cases}. \tag{8}$$

7. Drawing the interaction type

$$\begin{cases} \xi \le \dfrac{\mu_{foto}(E)}{\mu_{tot}(E)} \to photoeffect \\[2mm] \dfrac{\mu_{foto}(E)}{\mu_{tot}(E)} < \xi \le \dfrac{\mu_{foto}(E) + \mu_C(E)}{\mu_{tot}(E)} \to Compton's\ effect \\[2mm] \dfrac{\mu_{foto}(E) + \mu_C(E)}{\mu_{tot}(E)} < \xi \le \dfrac{\mu_{foto}(E) + \mu_C(E) + \mu_{par}(E)}{\mu_{tot}(E)} \to effect\ of\ pair\ production \\[2mm] \xi > \dfrac{\mu_{foto}(E) + \mu_C(E) + \mu_{par}(E)}{\mu_{tot}(E)} \to Rayleigh's\ effect \end{cases}. \tag{9}$$

8. For the case of photo-effect, go to the step 10.

9. For the case of Rayleigh scattering, drawing the secondary photons direction (the angles θ and φ). The energy of the photons are still the same: $E = E$. Go to the step 14.

10. Drawing the secondary electrons direction with the energy E (the angles θ_e and φ_e). Go to the step 12.

11. For the case of Compton scattering, drawing the azimuthal and polar angles θ and φ for the secondary photons.

12. Drawing the direction and the energy of secondary electrons (the angles θ_e and φ_e). Go to the step 13.

13. For the case of pair creation, drawing the azimuthal and polar angles θ and φ for secondary photons with energy E_γ=611 keV. Doubling photons weight factor: w=$2w$**.**

14. Drawing the direction and energy of the secondary electrons (the angles θ_e and φ_e).

15. Calculating the unit vector of the secondary electron direction:

$$\begin{cases} a_e = a\cos\theta_e - (b\sin\varphi_e - ac\cos\varphi_e)\sqrt{\dfrac{1-\cos\theta_e^2}{1-c^2}} \\[4mm] b_e = b\cos\theta_e + (a\sin\varphi_e + bc\cos\varphi_e)\sqrt{\dfrac{1-\cos\theta_e^2}{1-c^2}} \\[4mm] c_e = c\cos\theta_e - (1-c^2)\cos\varphi_e\sqrt{\dfrac{1-\cos\theta_e^2}{1-c^2}} \end{cases} . \tag{10}$$

16. Determining the point coordinates of hypothetical quantum exit from the scintillator as intersection point with the surface S by the straight line given by the formula:

$$\begin{cases} x_e = x + al_e \\ y_e = y + bl_e \\ z_e = z + cl_e \end{cases} , \tag{11}$$

where l_e is the distance from the photon interaction point (secondary electron creation) to the point of hypothetical secondary electron departure from the scintillator.

17. Calculating the energy transferred to scintillator material by the secondary electron using the continuous delay approximation [15]:

$$E_{e\,ab} = \min\{D(E_e)l_e, E_e\}. \tag{12}$$

18. Increasing the local absorbed energy adder by the registered photon energy: $E_{ab} = E_{ab} + E_{e\,ab}$.

19. For the case of photo-effect or $k > k_{max}$, go to the step 22.

20. Calculating the unit vector of new photon direction via the unit vector of the recent direction (the index *old*)

$$\begin{cases} a = a_{old}\cos\theta - (b_{old}\sin\varphi - a_{old}c_{old}\cos\varphi)\sqrt{\dfrac{1-\cos\theta^2}{1-c_{old}^2}} \\[4mm] b = b_{old}\cos\theta + (a_{old}\sin\varphi + b_{old}c_{old}\cos\varphi)\sqrt{\dfrac{1-\cos\theta^2}{1-c_{old}^2}} \\[4mm] c = c_{old}\cos\theta - (1-c_{old}^2)\cos\varphi\sqrt{\dfrac{1-\cos\theta^2}{1-c_{old}^2}} \end{cases} . \tag{13}$$

21. Go to the step 4.

22. Increasing the absorbed energy and absorbed energy square adders by the registered photons: $\sum E_{ab} = \sum E_{ab} + E_{e\,ab}$ and $\sum E_{ab}^2 = \sum E_{ab}^2 + E_{e\,ab}^2$.

23. Go to the step 1.

24. Calculating the mean value, the square of the absorbed energy and the accumulation coefficient of fluctuations:

$$\overline{E_{ab}} = \frac{\sum E_{ab}}{N}, \; \overline{E_{ab}^2} = \frac{\sum E_{ab}^2}{N}, \; \eta = \frac{\sqrt{\overline{E_{ab}^2}}}{\overline{E_{ab}}} \; . \tag{14}$$

26. The calculations end.

3. Verification of the Model Results

The results are similar to the data from the work [9-16]. As expected, mean and square values of registered photons absorbed energy are close to zero when scintillation detector thickness or radius approaching zero.

4. Conclusion

The offered method for modeling registration process of high-energy X-ray radiation has high efficiency. It can be used for estimation of X-ray radiation registrar parameters for systems of digital radiography and computer tomography.

5. Acknowledgements

References

[1]   Mathew V 2014 *Quality Magazine* Retrieved from http://www.qualitymag.com/articles/92208-industrial-digital-radiography

[2]   Li L *et al* 2016 *Applied Radiation and Isotopes* **114** 188–95 DOI: 10.1016/j.apradiso.2016.05.018

[3]   Hamm R W *and* Hamm M E (Eds) 2012 *Industrial accelerators and their applications* (Singapore: World Scientific)

[4]   Ueaska M *et al* 2014 *J. of Physics B: Atomic, Molecular and Optical Physics* **47** 234008 DOI: 10.1088/0953-4075/47/23/234008

[5]   Li Y *et al* 2003 *IEEE Nuclear Science Symposium Conference Record* **2** 8066819 DOI: 10.1109/NSSMIC.2003.1351949

[6]   Chakhlov S V et al 2016 *J. of Physics: Conf. Ser.* **671(1)** 012024 DOI: 10.1088/1742-6596/671/1/012024

[7]   Wells K *and* Bradley D A 2012 *Applied Radiation and Isotopes* **70** 1729–1746 DOI: 10.1016/j.apradiso.2012.01.011

[8]   Kasianov V A *et al* 2006 *Sensors & Systems* **3** 10−3

[9]   Zav'yalkin F M *and* Osipov S P 1985 *At Energ.* **59** 281–3 DOI: 10.1007/BF01123317

[10]   Zav'yalkin F M *and* Osipov S P 1986 *At Energ.* **60** 186−8 DOI: 10.1007/BF01371189

[11]   Broder D L *et al* (Eds) 1973 *Handbook on radiation protection for engineers* **1** (Moscow: Atomizdat) (In Russian)

[12]   Ali E S M *and* Rogers D W O 2011 *Physics in medicine and biology* **57** 31−50 DOI: 10.1088/0031-9155/57/1/31

[13]   Schiff L I 1951 *Physical review* **83** 252–3 DOI: 10.1103/PhysRev.83.252

[14]   *Gamma data for elements* Retrieved from http://www.ippe.ru/podr/abbn/libr/gdfe.php

[15]   *National Nuclear Data Center* Retrieved from http://www.nndc.bnl.gov

[16]   Mustafina R M *et al* 2016 *J. of Physics: Conf. Ser.* **671** DOI: 10.1088/1742-6596/671/1/012046